Eur. Phys. J. A **20**, 283–291 (2004)
DOI 10.1140/epja/i2003-10158-3

THE EUROPEAN PHYSICAL JOURNAL A

Electric and magnetic form factors of strange baryons

T. Van Cauteren[1,a], D. Merten[2], T. Corthals[1], S. Janssen[1], B. Metsch[2], H.-R. Petry[2], and J. Ryckebusch[1]

[1] Ghent University, Department of Subatomic and Radiation Physics, Proeftuinstraat 86, B-9000 Gent, Belgium
[2] Helmholtz-Institut für Strahlen- und Kernphysik, Nußallee 14-16, D-53115 Bonn, Germany

Received: 2 October 2003 /
Published online: 20 April 2004 – © Società Italiana di Fisica / Springer-Verlag 2004
Communicated by V. Vento

Abstract. Predictions for the electromagnetic form factors of the Λ, Σ and Ξ hyperons are presented. The numerical calculations are performed within the framework of the fully relativistic constituent-quark model developed by the Bonn group. The computed magnetic moments compare favorably with the experimentally known values. Most magnetic form factors $G_M(Q^2)$ can be parameterized in terms of a dipole with cutoff masses ranging from 0.79 to 1.14 GeV.

PACS. 11.10.St Bound and unstable states; Bethe-Salpeter equations – 12.39.Ki Relativistic quark model – 13.40.Gp Electromagnetic form factors

1 Introduction

Ever since the pioneering work by Murray Gell-Mann [1,2], Yuval Ne'eman [3] and George Zweig [4,5], the concept of *constituent quarks* (CQ) has become well accepted in hadronic physics. To date, constituent quarks are the effective degrees of freedom in many existing models for hadrons. They do not represent, however, the fundamental degrees of freedom of the theory of strong interactions, quantum chromodynamics (QCD). Usually, one connects the effective and fundamental degrees of freedom by noting that constituent quarks are conglomerates of quarks, antiquarks and gluons, such that the quantum numbers of the composed hadron depend only on those of the conglomerate. Thereby, one presumes that the quark and gluon degrees of freedom can be efficiently described by means of constituent quarks in the energy domain where the full QCD equations cannot be solved perturbatively. This procedure results in equations that are admittedly easier to handle than those obtained within the framework of nonperturbative QCD, but still carry all the complications connected with the (relativistic) treatment of a two- and three-body problem. The major justification for CQ models is their effectiveness in describing hadron spectra, symmetry properties and electromagnetic form factors. This work will focus on the latter quantities.

Meson photoproduction and scattering are primary tools to gain a deeper insight into the dynamics of baryon resonances. Fair descriptions of these data can be reached within the framework of isobar models. These models typically adopt hadrons and their resonances as effective degrees of freedom. Their finite size is modeled through the introduction of hadronic and electromagnetic form factors. With the eye on optimizing the agreement between calculations and data, the cutoff masses entering the form factors and the coupling constants are often treated as parameters. The underlying philosophy is that the fitted values can subsequently be compared to predictions from more fundamental models which explicitly account for the hadron substructure and dynamics. On the other hand, the coupling constants, computed in CQ models, could serve as input parameters into isobar descriptions of meson photoproduction processes, thereby establishing a more direct link between models for hadron structure and meson photoproduction and scattering experiments.

Attempts to describe meson production processes within the framework of a CQ model include the following ones. Zhao and Li *et al.* have used a (chiral) CQ model for baryons and quark-meson couplings to describe, *e.g.*, ω and η photoproduction on the proton [6,7]. Oh *et al.* [8] have investigated the contributions of direct knockout, diffractive and one-boson exchange processes in ϕ electroproduction. In ref. [9], a diquark-quark model has been used to calculate kaon photoproduction cross-sections. A dynamical approach to predict πN scattering amplitudes has been developed in refs. [10,11].

The work presented here finds its motivation in the development of a consistent description of kaon production processes $p(\gamma, K^+)Y$ and $p(e, e'K^+)Y$ [12–15], based on CQ degrees of freedom. New data for these processes have recently been released by the CLAS Collaboration at Jefferson Laboratory [16], by the LEPS Collaboration at

[a] e-mail: Tim.VanCauteren@UGent.be

SPring-8 [17] and by the SAPHIR Collaboration at ELSA in Bonn [18]. Also the GRAAL Collaboration in Grenoble [19] will provide extensive data sets for kaon photoproduction in the very near future. The abundant amount of new data calls for an appropriate theoretical treatment covering the complete data base. One of the major sources of theoretical uncertainties when modeling $p(e,e'K)Y$ reactions, is the Q^2-dependence of the electromagnetic form factors of the "strange" baryons [15]. In this work, theoretical predictions for these quantities will be presented.

In the resonance region, pion and eta photoproduction on the proton can be reasonably described within the framework of isobar models. For the pion channel, this success can be mainly attributed to the dominant role of the $\Delta(1232)$-resonance in the reaction dynamics. The large coupling of this resonance to the πN decay channel makes contributions of other reaction mechanisms seem like rather small perturbations. A similar role is played by the $S_{11}(1535)$-resonance in η photo- and electroproduction. In comparison to π and η production, kaon photo- and electroproduction are more difficult to treat, since there is no obvious dominant reaction mechanism, but several contributions compete. Furthermore, the threshold for production of strange $s\bar{s}$ pairs increases the energy scale to a domain in which isobar models could be expected to start losing their validity. A CQ model could provide an alternative approach, since its number of free parameters remains low, no matter how many resonances participate in the production mechanism. Also, CQs are supposed to be smaller in size than the hadron they represent [20]. Therefore, CQ models are expected to be valid up to larger energies and momentum transfers.

Many CQ approaches start off nonrelativistically and require relativistic corrections at some point. This procedure of relativizing certain aspects of the model usually involves some degree of arbitrariness. The CQ model which will be applied here, on the other hand, has been developed by the Bonn group [21–24] and is relativistically covariant in its inception. Yet, at the same time, it is linked to nonrelativistic models in a transparent way. The latter feature arises from the use of the instantaneous approximation and the CPT theorem which ensures that we arrive at the same number of bound states as nonrelativistic models [21]. In addition, an extended version of a harmonic-oscillator basis, which also serves as the starting point of many nonrelativistic CQ models is used. The Bonn CQ model is primarily based on the Bethe-Salpeter approach [25]. The quantities of physical interest can be obtained from integral equations which are solved numerically. Thereby, some freedom exists with respect to the plausible types of interactions between the constituent quarks. Preserving Lorentz covariance, which is mandatory for describing boosts consistently, it is assumed that the inter-quark forces do not depend on the components of the variables parallel to the total four-momentum of the baryon. In the rest frame, this means that the interactions are instantaneous or, in other words, independent of the energy components of the variables. This has the numerical advantage of reducing the integrations from eight to six dimensions when determining the Bethe-Salpeter amplitudes. The relativistic CQ model developed in Bonn adopts a typical linear confinement potential ($V_{\rm conf}$) supplemented by the 't Hooft instanton-induced interaction ($V_{\rm III}$). This approach allows one to use merely seven free parameters. They can be constrained by means of the mass spectra of strange and nonstrange baryons [22,23].

Previous work on electromagnetic form factors using the Bethe-Salpeter approach has been reported in ref. [26] for mesons and in ref. [27] for nonstrange baryons. An excellent description of the lowest pseudoscalar- and vector-meson elastic and transition form factors was obtained, except for the pion isotriplet, where the outcome was reasonable. The results on electromagnetic properties of the nonstrange baryons and baryon resonances are in quantitative agreement with the existing data up to the third resonance region ($W \leq 1.7$ GeV). It should be stressed that in many investigations, the covariant description of the dynamics turned out to be of the utmost importance [28].

This work focuses on computing the electric and magnetic form factors of strange baryons, as well as the electromagnetic form factors of the $\Sigma^0 \to \Lambda$ transition. In sect. 2, the Bethe-Salpeter (BS) formalism will be sketched. We will then turn our attention to electromagnetic form factors in sect. 3. The results of our numerical calculations will be presented in sect. 4. Whenever possible, we will compare our predictions with experimental data and previous CQ calculations.

2 Formalism

The Bethe-Salpeter (BS) formalism used in this work is described in great detail in refs. [21] and [27]. Here, we briefly recall its basic ingredients.

2.1 The Bethe-Salpeter equation (BSE)

In the model adopted here, the basic quantity describing a baryon is the three-quark BS amplitude:

$$\chi_{\bar{P},a_1,a_2,a_3}(x_1,x_2,x_3) \equiv \langle 0|T\big(\Psi_{a_1}(x_1)\Psi_{a_2}(x_2)\Psi_{a_3}(x_3)\big)|\bar{P}\rangle \ , \quad (1)$$

where T is the time-ordering operator acting on the Heisenberg quark field operators Ψ_{a_i}, and $\bar{P}$ is the total four-momentum of the baryon with $\bar{P}_\mu \bar{P}^\mu = M^2$. The a_i denote the quantum numbers in Dirac, flavor and color space. The Fourier transform of the above quantity is defined by

$$\chi_{\bar{P},a_1,a_2,a_3}(x_1,x_2,x_3) = e^{-i\bar{P}.X}\chi_{\bar{P}}(\xi,\eta)$$
$$\equiv e^{-i\bar{P}.X}\int \frac{\mathrm{d}^4p_\xi}{(2\pi)^4}\frac{\mathrm{d}^4p_\eta}{(2\pi)^4}e^{-ip_\xi.\xi}e^{-ip_\eta.\eta}\chi_{\bar{P}}(p_\xi,p_\eta) \ , \quad (2)$$

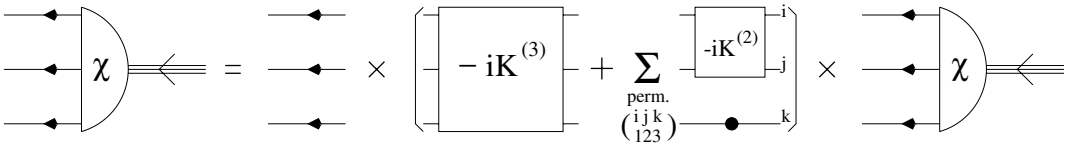

Fig. 1. The BS equation in a schematic form. Arrows represent quark propagators, the filled dot denotes an inverse propagator.

where the scalar product of two four-vectors is given by the convention $a\cdot b = a_\mu b^\mu = a^0 b^0 - \boldsymbol{a}\cdot\boldsymbol{b}$. The standard definition of the Jacobi coordinates and momenta is adopted:

$$\begin{cases} X = \frac{1}{3}(x_1 + x_2 + x_3) \,, \\ \xi = x_1 - x_2 \,, \\ \eta = \frac{1}{2}(x_1 + x_2 - 2x_3) \,, \end{cases} \tag{3a}$$

and

$$\begin{cases} P = p_1 + p_2 + p_3 \,, \\ p_\xi = \frac{1}{2}(p_1 - p_2) \,, \\ p_\eta = \frac{1}{3}(p_1 + p_2 - 2p_3) \,. \end{cases} \tag{3b}$$

From eq. (2) it becomes clear that the total momentum $\bar{P}$ of the baryon enters the definition of the BS amplitude only parametrically and not as a variable, thereby naturally obeying the symmetry requirement of translational invariance.

The so-called BS amplitude $\chi_{\bar{P}} \equiv \chi_{\bar{P}}(p_\xi, p_\eta)$ is the solution to the BS equation [25] which, in momentum space, can be schematically written as

$$\chi_{\bar{P}} = -iG_{0\bar{P}} \left(K^{(3)}_{\bar{P}} + \bar{K}^{(2)}_{\bar{P}} \right) \chi_{\bar{P}} \,. \tag{4}$$

Here, the arguments and integrals over dummy arguments have been dropped. Its Feynman-diagram analogue is depicted in fig. 1. This equation can be obtained from considering the six-point Green's function, a quantity which depends on the total four-momentum squared $P_\mu P^\mu$ and possesses poles at the masses M^2 of the 3-quark bound states. The residue at these poles corresponds to the product of the BS amplitude and its adjoint.

The quantity $G_{0\bar{P}}$ in eq. (4) is the direct product of the dressed propagators of the three quarks:

$$\begin{aligned} G_{0\bar{P}}(p_\xi, p_\eta; p'_\xi, p'_\eta) = {} & S^1_{\mathrm{F}} \left(\frac{1}{3}P + p_\xi + \frac{1}{2}p_\eta \right) \\ & \otimes S^2_{\mathrm{F}} \left(\frac{1}{3}P - p_\xi + \frac{1}{2}p_\eta \right) \otimes S^3_{\mathrm{F}} \left(\frac{1}{3}P - p_\eta \right) \\ & \times (2\pi)^4 \delta^{(4)} \left(p_\xi - p'_\xi \right) (2\pi)^4 \delta^{(4)} \left(p_\eta - p'_\eta \right) \,. \end{aligned} \tag{5}$$

These propagators are approximated by the propagators of free constituent quarks. Therefore, we adopt the form

$$S^i_{\mathrm{F}}(p_i) = \frac{i}{\not{p}_i - m_i + i\epsilon} \,, \tag{6}$$

where m_i is the effective mass of the i-th constituent quark. The quantity denoted by $K^{(3)}_{\bar{P}}$ is the three-particle irreducible interaction kernel. Further, $\bar{K}^{(2)}_{\bar{P}}$ is the sum of two-particle irreducible interaction kernels, each multiplied by the inverse of the propagator of the spectator quark:

$$\begin{aligned} \bar{K}^{(2)}_{\bar{P}} \left(p_\xi, p_\eta; p'_\xi, p'_\eta \right) = {} & K^{(2)}_{(\frac{2}{3}P + p_\eta)} \left(p_\xi, p'_\xi \right) \\ & \otimes \left[S^3_{\mathrm{F}} \left(\frac{1}{3}P - p_\eta \right) \right]^{-1} \times (2\pi)^4 \delta^{(4)} \left(p_\eta - p'_\eta \right) \\ & + \text{cycl. perm. in quarks (123)} \,. \end{aligned} \tag{7}$$

In the case of instantaneous forces, $K^{(3)}_{\bar{P}}$ and $K^{(2)}_{p_i+p_j}$ are independent of the component of the Jacobi momenta parallel to the baryon four-momentum $\bar{P}$, as was already discussed in sect. 1. In the c.o.m. frame, this condition implies that there is no dependence on the energy components:

$$K^{(3)}_P \left(p_\xi, p_\eta; p'_\xi, p'_\eta \right) \Big|_{P=(M,\mathbf{0})} = V^{(3)} \left(\boldsymbol{p}_\xi, \boldsymbol{p}_\eta; \boldsymbol{p}'_\xi, \boldsymbol{p}'_\eta \right) \,, \tag{8a}$$

$$K^{(2)}_{(\frac{2}{3}P + p_\eta)} \left(p_\xi, p'_\xi \right) \Big|_{P=(M,\mathbf{0})} = V^{(2)} \left(\boldsymbol{p}_\xi, \boldsymbol{p}'_\xi \right) \,. \tag{8b}$$

We should mention here that whenever a quantity is to be evaluated in the rest frame of the baryon, we will indicate this by the index M, to make it clear that in this case $\bar{P} = (M, \mathbf{0})$.

The potentials used in our calculations are those of model $\mathcal{A}$ of ref. [22]. The three-particle interaction is given by a *confinement* potential $V^{(3)}_{\mathrm{conf}}$ which rises linearly with the sum of the distances between the three CQs. The two-particle residual interaction is the *'t Hooft Instanton Induced Interaction* $V^{(2)}_{\mathrm{III}}$, which acts between pairs of quarks that have antisymmetric spin, flavor and color wave functions.

2.2 Reduction to the Salpeter equation

Solving eq. (4) can be simplified by exploiting the instantaneous property of the interaction kernels. Indeed, the integration over the energy components of the Jacobi momenta can be performed analytically. This gives rise to a new object Φ_M, the Salpeter amplitude, which can be directly obtained from the full BS amplitude :

$$\Phi_M \left(\boldsymbol{p}_\xi, \boldsymbol{p}_\eta \right) = \int \frac{\mathrm{d}p^0_\xi}{(2\pi)} \frac{\mathrm{d}p^0_\eta}{(2\pi)} \chi_M \left((p^0_\xi, \boldsymbol{p}_\xi), (p^0_\eta, \boldsymbol{p}_\eta) \right) \,. \tag{9}$$

This definition is only workable in the special case that no genuine two-particle irreducible interactions contribute,

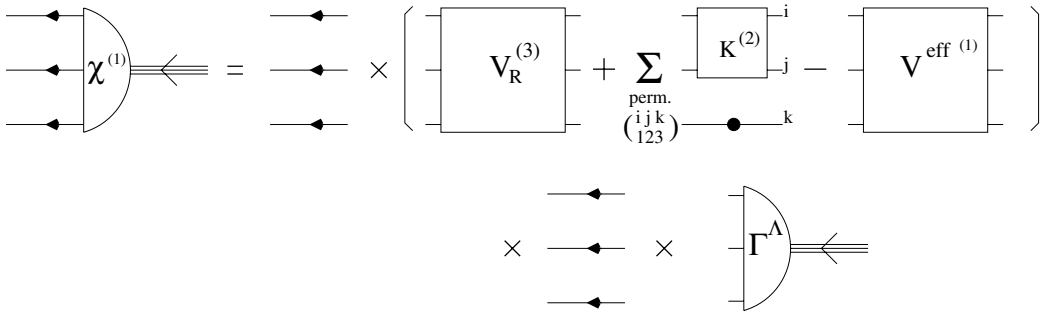

Fig. 2. The reconstruction of the BS amplitude from the vertex function according to eq. (16).

e.g. for the decuplet baryons which have symmetric spin wave functions. For the octet baryons, approximations are needed, as is explained in the appendix of ref. [27] and in ref. [21]. There, it is pointed out that for reconstructing the Bethe-Salpeter amplitude (1), it suffices to compute the projection of the Salpeter amplitude (9) onto the purely positive-energy and negative-energy states. This can be accomplished in the standard manner by introducing the energy projection operators:

$$\Lambda_i^{\pm}(\boldsymbol{p}_i) = \frac{\omega_i(\boldsymbol{p}_i)\,\mathbb{1} \pm H_i(\boldsymbol{p}_i)}{2\omega_i(\boldsymbol{p}_i)}\,, \tag{10}$$

where $\omega_i(\boldsymbol{p}_i) = \sqrt{m_i^2 + |\boldsymbol{p}_i|^2}$ denotes the energy and

$$H_i(\boldsymbol{p}_i) = \gamma^0(\boldsymbol{\gamma}\cdot\boldsymbol{p}_i + m_i) \tag{11}$$

is the free Hamiltonian of the i-th quark. With the above definition, we define the projected Salpeter amplitude as

$$\begin{aligned}\Phi_M^{\Lambda}(\boldsymbol{p}_\xi,\boldsymbol{p}_\eta) &= \left(\Lambda^{+++}(\boldsymbol{p}_\xi,\boldsymbol{p}_\eta) + \Lambda^{---}(\boldsymbol{p}_\xi,\boldsymbol{p}_\eta)\right)\\ &\times \int \frac{\mathrm{d}p_\xi^0}{(2\pi)}\frac{\mathrm{d}p_\eta^0}{(2\pi)}\chi_M\left((p_\xi^0,\boldsymbol{p}_\xi),(p_\eta^0,\boldsymbol{p}_\eta)\right)\,,\end{aligned} \tag{12}$$

where $\Lambda^{+++}(\boldsymbol{p}_\xi,\boldsymbol{p}_\eta) = \Lambda_1^+(\boldsymbol{p}_1)\otimes\Lambda_2^+(\boldsymbol{p}_2)\otimes\Lambda_3^+(\boldsymbol{p}_3)$ and $\Lambda^{---}(\boldsymbol{p}_\xi,\boldsymbol{p}_\eta) = \Lambda_1^-(\boldsymbol{p}_1)\otimes\Lambda_2^-(\boldsymbol{p}_2)\otimes\Lambda_3^-(\boldsymbol{p}_3)$.

The Salpeter equation is now given by

$$\begin{aligned}\Phi_M^{\Lambda}(\boldsymbol{p}_\xi,\boldsymbol{p}_\eta) &= \left[\frac{\Lambda^{+++}(\boldsymbol{p}_\xi,\boldsymbol{p}_\eta)}{M-\Omega(\boldsymbol{p}_\xi,\boldsymbol{p}_\eta)+i\varepsilon}\right.\\ &\left.+\frac{\Lambda^{---}(\boldsymbol{p}_\xi,\boldsymbol{p}_\eta)}{M+\Omega(\boldsymbol{p}_\xi,\boldsymbol{p}_\eta)-i\varepsilon}\right]\gamma^0\otimes\gamma^0\otimes\gamma^0\\ &\times\int\frac{\mathrm{d}^3p'_\xi}{(2\pi)^3}\frac{\mathrm{d}^3p'_\eta}{(2\pi)^3}V^{(3)}\left(\boldsymbol{p}_\xi,\boldsymbol{p}_\eta;\boldsymbol{p}'_\xi,\boldsymbol{p}'_\eta\right)\Phi_M^{\Lambda}\left(\boldsymbol{p}'_\xi,\boldsymbol{p}'_\eta\right)\\ &+\left[\frac{\Lambda^{+++}(\boldsymbol{p}_\xi,\boldsymbol{p}_\eta)}{M-\Omega(\boldsymbol{p}_\xi,\boldsymbol{p}_\eta)+i\varepsilon}-\frac{\Lambda^{---}(\boldsymbol{p}_\xi,\boldsymbol{p}_\eta)}{M+\Omega(\boldsymbol{p}_\xi,\boldsymbol{p}_\eta)-i\varepsilon}\right]\\ &\times\int\frac{\mathrm{d}^3p'_\xi}{(2\pi)^3}\left[\left[\gamma^0\otimes\gamma^0V^{(2)}\left(\boldsymbol{p}_\xi,\boldsymbol{p}'_\xi\right)\right]\otimes\mathbb{1}\right]\Phi_M^{\Lambda}\left(\boldsymbol{p}'_\xi,\boldsymbol{p}_\eta\right)\\ &+\text{ cycl. perm. in quarks (123)}\,,\end{aligned} \tag{13}$$

where $\Omega(\boldsymbol{p}_\xi,\boldsymbol{p}_\eta)$ is the sum of the energies of the three constituent quarks:

$$\Omega = \sum_{i=1}^{3}\omega_i = \sum_{i=1}^{3}\sqrt{|\boldsymbol{p}_i|^2+m_i^2}\,. \tag{14}$$

Once the Salpeter equation (13) is solved, the vertex function Γ_M^{Λ} can be constructed:

$$\begin{aligned}\Gamma_M^{\Lambda}(\boldsymbol{p}_\xi,\boldsymbol{p}_\eta) &= -i\int\frac{\mathrm{d}^3p'_\xi}{(2\pi)^3}\frac{\mathrm{d}^3p'_\eta}{(2\pi)^3}\Big[V_{\Lambda}^{(3)}\left(\boldsymbol{p}_\xi,\boldsymbol{p}_\eta;\boldsymbol{p}'_\xi,\boldsymbol{p}'_\eta\right)\\ &+V_M^{\mathrm{eff}(1)}\left(\boldsymbol{p}_\xi,\boldsymbol{p}_\eta;\boldsymbol{p}'_\xi,\boldsymbol{p}'_\eta\right)\Big]\Phi_M^{\Lambda,(1)}\left(\boldsymbol{p}'_\xi,\boldsymbol{p}'_\eta\right)\,.\end{aligned} \tag{15}$$

This vertex function describes how the three CQs couple to form a baryon, and in first order can be related to the BS amplitude through

$$\chi_{\bar{P}} \approx \chi_{\bar{P}}^{(1)} = \left[G_{0\bar{P}}\left(V_R^{(3)} + \bar{K}_{\bar{P}}^{(2)} - V_{\bar{P}}^{\mathrm{eff}(1)}\right)G_{0\bar{P}}\right]\Gamma_{\bar{P}}^{\Lambda}\,, \tag{16}$$

of which a diagram is shown in fig. 2.

In eqs. (15) and (16), $V_{\Lambda}^{(3)} = \bar{\Lambda}V_R^{(3)}\Lambda$, where $\bar{\Lambda} = \gamma^0\otimes\gamma^0\otimes\gamma^0\Lambda\gamma^0\otimes\gamma^0\otimes\gamma^0$, is that part of the three-body potential which couples only to purely positive-energy and negative-energy components of the amplitudes. $V_R^{(3)} = V^{(3)} - V_{\Lambda}^{(3)}$ is the remaining part which couples to the mixed-energy components. $V_{\bar{P}}^{\mathrm{eff}(1)}$ is a first-order approximation of an effective potential with three-body structure which parameterizes the two-body interaction [21,27]. Further, $\bar{K}_{\bar{P}}^{(2)}$ is defined in eqs. (7) and (8b).

2.3 Current matrix elements

Once the BS amplitudes and vertex functions have been determined, the current matrix elements can be computed through the following definition:

$$\langle\bar{P}|j^{\mu}(x)|\bar{P}'\rangle = \langle\bar{P}|\bar{\Psi}(x)\hat{q}\gamma^{\mu}\Psi(x)|\bar{P}'\rangle\,, \tag{17}$$

where Ψ and $\hat{q}$ are the constituent-quark field and charge operator. The above matrix element can be expressed in terms of the objects defined in sects. 2.1 and 2.2. Via the

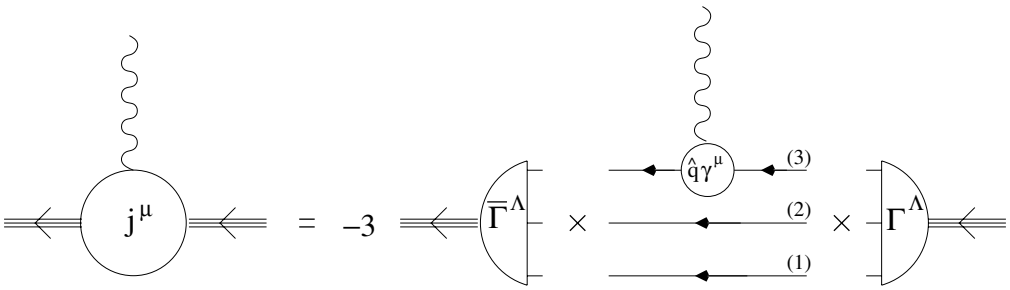

Fig. 3. Feynman diagram showing the coupling of the photon to the third CQ as in eq. (18). The other two CQs are spectators.

calculation of the six-point and eight-point Green's functions and residue arguments, it can be shown that in the c.o.m. frame of the incoming baryon [27]

$$\begin{aligned}\langle \bar{P}|j^{\mu}(0)|M\rangle \;\simeq -3 \int \frac{\mathrm{d}^4p_\xi}{(2\pi)^4}\frac{\mathrm{d}^4p_\eta}{(2\pi)^4} \\ \times \bar{\Gamma}^{\Lambda}_{\bar{P}}\left(p_\xi, p_\eta - \frac{2}{3}q\right) S^1_{\mathrm{F}}\left(\frac{1}{3}M + p_\xi + \frac{1}{2}p_\eta\right) \\ \otimes S^2_{\mathrm{F}}\left(\frac{1}{3}M - p_\xi + \frac{1}{2}p_\eta\right) \otimes S^3_{\mathrm{F}}\left(\frac{1}{3}M - p_\eta + q\right) \\ \times \hat{q}\gamma^{\mu} S^3_{\mathrm{F}}\left(\frac{1}{3}M - p_\eta\right) \Gamma^{\Lambda}_{M}\left(\boldsymbol{p}_\xi, \boldsymbol{p}_\eta\right) \;, \quad (18)\end{aligned}$$

where q is the (incoming) photon four-momentum and $\hat{q}$ is the charge operator working on the third CQ only. Further, $\bar{\Gamma}^{\Lambda}_{\bar{P}}$ is the adjoint vertex function and is calculated in the c.o.m. system according to

$$\bar{\Gamma}^{\Lambda}_{M} = -\left(\Gamma^{\Lambda}_{M}\right)^{\dagger}\gamma^0 \otimes \gamma^0 \otimes \gamma^0 \;. \quad (19)$$

Under a Lorentz boost, the vertex function transforms as [24]

$$\begin{aligned}&\Gamma_{\bar{P}}\left(p_\xi, p_\eta - \frac{2}{3}q\right) = \\ &S^1_{\Lambda} \otimes S^2_{\Lambda} \otimes S^3_{\Lambda}\Gamma_{\Lambda^{-1}\bar{P}}\left(\Lambda^{-1}p_\xi, \Lambda^{-1}\left(p_\eta - \frac{2}{3}q\right)\right) \;, \quad (20)\end{aligned}$$

with Λ the boost matrix and S^i_{Λ} the corresponding boost operator acting on the i-th quark. Equation (18) is a consistent lowest-order approximation of the current matrix element. We refer to refs. [24] and [27] for more details and to fig. 3 for a schematic representation of eq. (18). The integration over the energy variables can be performed analytically. In the remaining integral over $\boldsymbol{p}_\xi$ and $\boldsymbol{p}_\eta$, the azimuthal dependence can be reduced to $(\phi_\xi - \phi_\eta)$, leaving one with five-dimensional integrals, which are computed numerically.

3 Form factors

In sect. 4, results for the elastic and transition electromagnetic form factors of the octet baryons with a nonvanishing strangeness quantum number will be presented. Here, we briefly discuss our conventions regarding the connection between form factors and current matrix elements.

3.1 Elastic form factors

The strength with which real and virtual photons couple to baryons can be quantified in different ways. For the elastic processes, where the incoming and the outgoing baryon are identical, we will compute the Sachs form factors. We define the vertex function Γ^{μ} between a baryon and a photon as

$$\begin{aligned}&\langle B, \bar{P}', \lambda'|j^{\mu}(0)|B, \bar{P}, \lambda\rangle = e\bar{u}_{\lambda'}(\bar{P}')\Gamma^{\mu}u_{\lambda}(\bar{P}) \\ &= e\bar{u}_{\lambda'}(\bar{P}')\left[\gamma^{\mu}F^B_1(Q^2) + \frac{i\sigma^{\mu\nu}q_\nu}{2M}F^B_2(Q^2)\right]u_{\lambda}(\bar{P}) \;, \quad (21)\end{aligned}$$

where B denotes the baryon under investigation, $\lambda^{(')}$ the baryon helicity, $\bar{P}^{(')}$ the baryon on-shell four-momentum and $u_\lambda(\bar{P})$ a Dirac spinor, normalized according to

$$\bar{u}_{\lambda'}(\bar{P})u_{\lambda}(\bar{P}) = 2M\delta_{\lambda\lambda'} \;. \quad (22)$$

The functions F^B_1 and F^B_2 are the Dirac and Pauli form factors and depend only on $Q^2 = -q^2$, where q is the four-momentum carried by the photon. The Sachs form factors are defined in the standard fashion,

$$G^B_E(Q^2) = F^B_1(Q^2) - \frac{Q^2}{4M^2}F^B_2(Q^2) \;, \quad (23a)$$

$$G^B_M(Q^2) = F^B_1(Q^2) + F^B_2(Q^2) \;. \quad (23b)$$

The equations connecting the Sachs form factors to the current matrix elements in the rest frame of the incoming baryon read

$$G^B_E(Q^2) = \frac{\langle B, \bar{P}', \frac{1}{2}|j_0(0)|B, \bar{M}, \frac{1}{2}\rangle}{\sqrt{4M^2 + Q^2}} \;, \quad (24a)$$

$$G^B_M(Q^2) = \frac{\langle B, \bar{P}', \frac{1}{2}|j_+(0)|B, \bar{M}, -\frac{1}{2}\rangle}{2\sqrt{Q^2}} \;. \quad (24b)$$

Measurements of the magnetic moments for the strange baryons represent a direct test of the calculations which will be presented here. These values should be compared to the values of the magnetic Sachs form factors at $Q^2 = 0$. From the slope of the form factors at $Q^2 = 0$, the electric and magnetic mean-square radii of the baryons can be deduced from

$$\langle r^2\rangle = -6\frac{1}{G(0)}\frac{\mathrm{d}G(Q^2)}{\mathrm{d}Q^2}\bigg|_{Q^2=0} \;, \quad (25)$$

if the form factor does not go to zero for $Q^2 \to 0$, and

$$\langle r^2 \rangle = -6 \frac{\mathrm{d}G(Q^2)}{\mathrm{d}Q^2}\bigg|_{Q^2=0} , \tag{26}$$

if the form factor vanishes at $Q^2 = 0$. Two recent measurements at CERN [29] and Fermilab [30] provided the first values for the electric mean-square radius of the Σ^- hyperon. To our knowledge, the Σ^- is the only hyperon for which such information is presently available.

3.2 Transition form factors

When describing electromagnetic transitions at vertex level, at a certain point, one is forced to make a choice as to what operatorial form to use. The only condition which should be obeyed is the Ward identity $q_\mu \Gamma^\mu = 0$. A general form for the vertex function for spin-(1/2) baryons corresponding with $\gamma^* + B^* \longrightarrow B$ transitions, is

$$\Gamma^\mu = F_1^{B^*B}(Q^2) \left(\gamma^\mu + \frac{q^\mu q^\nu}{Q^2} \gamma_\nu \right) + \frac{F_2^{B^*B}(Q^2) \kappa_{B^*B}}{2M_p} i\sigma^{\mu\nu} q_\nu , \tag{27}$$

with M_p the proton mass, $F_1^{B^*B}(Q^2)$ and $F_2^{B^*B}(Q^2)$ the two transition form factors, belonging to parts of the vertex that obey the Ward identity individually, and κ_{B^*B} the transition magnetic moment in units of the nuclear magneton μ_N. In the rest frame of the incoming baryon B^*, we get the following equations for the transition form factors:

$$eF_1^{B^*B}(Q^2) = \frac{Q^2}{Q^+\sqrt{Q^-}} \times \left[\frac{M+M^*}{|\boldsymbol{P'}|} \mathcal{M}_0 - \frac{1}{2} \mathcal{M}_+ \right] , \tag{28a}$$

$$\frac{e\kappa_{B^*B} F_2^{B^*B}(Q^2)}{2M_p} = \frac{-1}{Q^+\sqrt{Q^-}} \times \left[\frac{Q^2}{|\boldsymbol{P'}|} \mathcal{M}_0 + \frac{M+M^*}{2} \mathcal{M}_+ \right] , \tag{28b}$$

with M^* and M the mass of incoming and outgoing baryons, respectively, $|\boldsymbol{P'}|$ the magnitude of the three-momentum of the outgoing baryon, $Q^\pm = Q^2 + (M^* \pm M)^2$ and

$$\mathcal{M}_0 = \left\langle B, \bar{P}', \frac{1}{2} \middle| j_0(0) \middle| B^*, \bar{M}^*, \frac{1}{2} \right\rangle , \tag{29a}$$

$$\mathcal{M}_+ = \left\langle B, \bar{P}', \frac{1}{2} \middle| \left(-j^1(0) - i.j^2(0) \right) \middle| B^*, \bar{M}^*, -\frac{1}{2} \right\rangle . \tag{29b}$$

Hereby, we have implicitly adopted the axial gauge $\boldsymbol{\epsilon} \cdot \boldsymbol{q} = 0$, where $\boldsymbol{\epsilon}$ is the photon polarization three-vector.

With these definitions for the transition form factors, $F_1^{B^*B}(0)$ gives the *transition* charge and κ_{B^*B} is the transition magnetic moment, since $F_2^{B^*B}(0) = 1$ by convention.

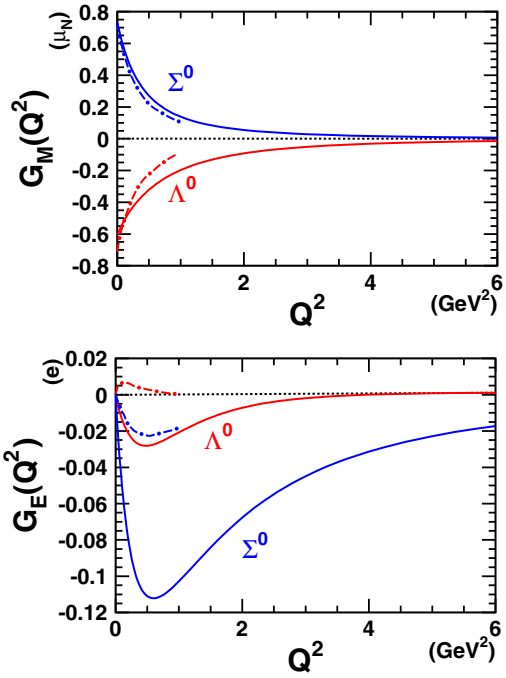

Fig. 4. Calculated magnetic (top) and electric (bottom) form factors of the Λ and Σ^0 hyperons. The dot-dashed curves are the predictions from ref. [31].

4 Results

In this section, results for the computed electric and magnetic form factors of the strange particles belonging to the baryon octet will be presented. We will discuss the elastic and the $\Sigma^0 \to \Lambda$ transition form factors. Comparisons with other calculations will be made. In ref. [31], Kim *et al.* present calculations for the elastic form factors of the ground-state octet baryons up to $Q^2 = 1.0$ GeV^2 within the framework of the chiral quark/soliton model. Kubis *et al.* have computed electric and magnetic form factors of the hyperons for $Q^2 < 0.2$ GeV^2 in the framework of heavy-baryon chiral perturbation theory (HB) in ref. [32] and later extended their model to fourth order [33] to recalculate the electric form factors of the baryon octet and the $\Sigma^0 \to \Lambda$ transition form factor $F_1^{B^*B}(Q^2)$ for $Q^2 < 0.3$ GeV^2. In the same article, relativistic baryon chiral perturbation employing infrared regulators (IR) is used and shown to have predictive value. Since these investigations are confined to small values for Q^2, we will only compare our results for the magnetic moments (table 1) and the mean-square radii (table 2) with the HB and IR results. We will also confront our predictions with those presented in ref. [34], where results are shown of CQ calculations based on a Goldstone-boson exchange (GBE) quark-quark interaction [35,36] and a one-gluon exchange (OGE) interaction [37,38].

In fig. 4, our results for the neutral single-strange baryons are displayed. The computed Q^2-dependence of the magnetic form factors of the Σ^0 and Λ hyperons nicely

Table 1. Magnetic moments of strange baryons in units of μ_N. The notation GBE/OGE (HB/IR) refers to the two different models discussed in ref. [34] ([33]). In ref. [33], only the transition magnetic moment for $\Sigma^0 \to \Lambda$ is a real prediction. Experimental values are taken from ref. [40], except for $\mu_{\Sigma^0} = (\mu_{\Sigma^+} + \mu_{\Sigma^-})/2$, for which isospin invariance is used. For the $\Sigma^0 \to \Lambda$ transition, the absolute value is given.

Baryon	$\mu_Y^{\rm exp}$	$\mu_Y^{\rm calc}$	$\mu_Y^{[31]}$	$\mu_{Y\ ({\rm GBE/OGE})}^{[34]}$	$\mu_{Y\ ({\rm HB/IR})}^{[33]}$
$\Lambda^0(1116)$	-0.613 ± 0.004	-0.61	-0.77	$-0.59/-0.59$	exp.
$\Sigma^+(1189)$	2.458 ± 0.010	2.47	2.42	2.34/2.20	exp.
$\Sigma^0(1189)$	0.649	0.73	0.75	0.70/0.66	exp.
$\Sigma^-(1189)$	-1.160 ± 0.025	-0.99	-0.92	$-0.94/-0.89$	exp.
$\lvert\Sigma^0 \to \Lambda\rvert$	1.61 ± 0.08	1.41	1.51	–	1.46/1.61
$\Xi^0(1315)$	-1.250 ± 0.014	-1.33	-1.64	$-1.27/-1.27$	exp.
$\Xi^-(1315)$	-0.6507 ± 0.0025	-0.57	-0.68	$-0.67/-0.57$	exp.

Table 2. Magnetic mean-square radii of strange baryons in units of fm^2. All magnetic form factors resemble dipoles, except for the Σ^-, and our fitted value for the cutoff mass is given. The notation HB/IR refers to the two models presented in ref. [33].

Baryon	$\langle r_M^2\rangle^{\rm calc}$	$\langle r_M^2\rangle^{[31]}$	$\langle r_M^2\rangle^{[33]}_{\rm (HB/IR)}$	Λ_M (GeV)
$\Lambda^0(1116)$	0.40	0.70	0.30/0.48	1.14
$\Sigma^+(1189)$	0.69	0.71	0.74/0.80	0.79
$\Sigma^0(1189)$	0.60	0.70	0.20/0.45	0.88
$\Sigma^-(1189)$	0.81	0.74	1.33/1.20	–
$\Sigma^0 \to \Lambda$	1.96	–	0.60/0.72	0.82
$\Xi^0(1315)$	0.47	0.75	0.44/0.61	0.94
$\Xi^-(1315)$	0.38	0.51	0.44/0.50	1.03

follows that of a dipole,

$$G(Q^2) = \frac{G(0)}{\left(1 + \frac{Q^2}{\Lambda^2}\right)^2}\ , \qquad (30)$$

with cutoff masses $\Lambda_M = 0.88$ GeV and 1.14 GeV, respectively (table 2). Their values at $Q^2 = 0$ are the magnetic moments $\mu_{\Sigma^0} = 0.73$ and $\mu_\Lambda = -0.61$ in units of the nuclear magneton μ_N, which are very realistic (table 1). The electric form factors in the bottom panel of fig. 4 have the opposite sign in comparison with the neutron electric form factor. This can be attributed to the heavier s-quark in the hyperons, which has a higher probability of residing near the center of mass of the hyperon, making the electric density negative at small r, whereas it is positive for the neutron [39]. The predicted negative values for G_E for the Σ^0 and Λ, are in contradiction with the results from refs. [31] and [33]. Kim *et al.* predict a positive G_E for the Λ and Kubis *et al.* predict a negative mean-square radius for the Σ^0 hyperon (table 3). It should also be noted that for neutral hyperons, our results for the electric form factors are about a factor of five larger in magnitude than those of ref. [31]. This suggests that in our model, there is a higher charge density near the center of mass of the neutral hyperon than in the chiral quark/soliton model.

Our predictions for the charged single-strange baryons $\Sigma^\pm$ are shown in fig. 5. Again, the results for the magnetic moments $\mu_{\Sigma^+} = 2.47\ \mu_N$ and $\mu_{\Sigma^-} = -0.99\ \mu_N$ are in excellent agreement with experiment (table 1). Whilst the magnetic form factor of the Σ^+ resembles a dipole with cutoff $\Lambda_M = 0.79$ GeV, the one for the Σ^- drops relatively fast and even changes sign at $Q^2 \approx 1.6$ GeV, remaining small at high Q^2. A similar qualitative behavior is observed for the electric form factor of the Σ^+, changing sign at $Q^2 \approx 1.1$ GeV^2. For $Q^2 > 2.6$ GeV^2, the form factors of Σ^+ and Σ^- become practically indistinguishable. Inspecting fig. 5, it is clear that our predictions for the magnetic form factors agree remarkably well with those of the chiral quark/soliton model at low values of Q^2 [31].

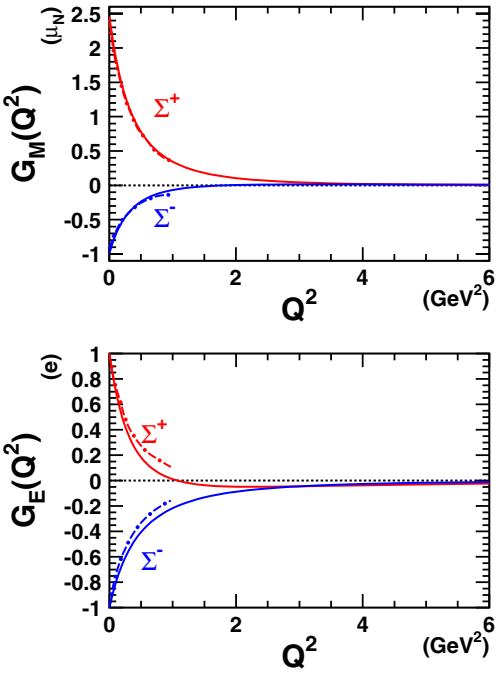

Fig. 5. Calculated magnetic and electric form factors of the Σ^+ and Σ^- hyperons. The dot-dashed curves are the predictions from ref. [31].

To our knowledge, for the electric mean-square radius of the Σ^- hyperon, the following experimental values are presently available:

$$\langle r_E^2\rangle_{\Sigma^-} = 0.60 \pm 0.08\ ({\rm stat.})\ \pm 0.08\ ({\rm syst.})\ {\rm fm}^2 \qquad (31)$$

Table 3. Electric mean-square radii of strange baryons in units of fm^2. The same conventions as in tables 1 and 2.

Baryon	$\langle r_E^2\rangle^{\rm exp}$	$\langle r_E^2\rangle^{\rm calc}$	$\langle r_E^2\rangle^{[31]}$	$\langle r_E^2\rangle^{[33]}_{\rm (HB/IR)}$	$\langle r_E^2\rangle^{[34]}_{\rm (GBE/OGE)}$	Λ_E (GeV)
$\Lambda^0(1116)$	–	0.038	−0.04	0.00/0.11	–	–
$\Sigma^+(1189)$	–	0.79	0.79	0.72/0.60	–	–
$\Sigma^0(1189)$	–	0.150	0.02	$-0.08/-0.03$	–	–
$\Sigma^-(1189)$	$0.60^{[30]}/0.91^{[29]}$	0.49	0.75	0.88/0.67	0.49/0.44	0.93
$\Sigma^0\to\Lambda$	–	−0.120	–	−0.09/0.03	–	–
$\Xi^0(1315)$	–	0.140	−0.06	0.08/0.13	–	–
$\Xi^-(1315)$	–	0.47	0.72	0.75/0.49	–	0.93

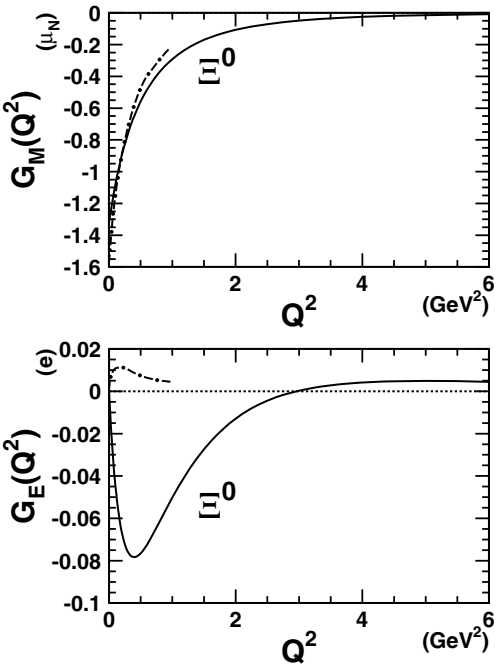

Fig. 6. Calculated magnetic and electric form factors of the Ξ^0 hyperon. The dot-dashed curves are the predictions from ref. [31].

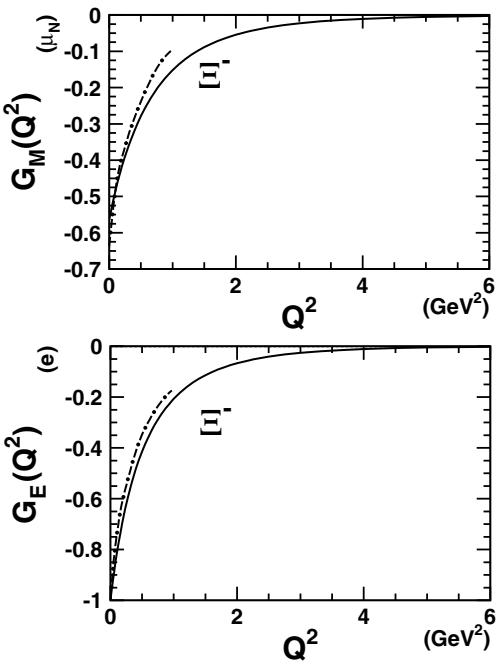

Fig. 7. Calculated magnetic and electric form factors of the Ξ^- hyperon. The dot-dashed curves are the predictions from ref. [31].

from ref. [30], and

$$\langle r_E^2\rangle_{\Sigma^-} = 0.91 \pm 0.32\ (\text{stat.})\ \pm 0.40\ (\text{syst.})\ \text{fm}^2 \quad (32)$$

from ref. [29]. Our prediction $\langle r_E^2\rangle_{\Sigma^-} = 0.49$ fm^2 (table 3) is compatible with both these values.

The experimental information regarding the Ξ doublet is scarce. To complete the description of ground-state hyperons, we have calculated its elastic form factors. The form factors of the Ξ^0 are displayed in fig. 6. The $G_E(Q^2)$ changes sign about $Q^2 = 3.0$ GeV^2 and $G_M(Q^2)$ can be nicely fitted with a dipole with $\Lambda_M = 0.94$ GeV and magnetic moment $\mu_{\Xi^0} = -1.33\ \mu_N$. Again, this value for μ_{Ξ^0} is in good agreement with the experimentally determined value (table 1). The Ξ^- exhibits dipole-like behavior in both $G_E(Q^2)$ and $G_M(Q^2)$ (fig. 7) with cutoffs $\Lambda_E = 0.93$ GeV and $\Lambda_M = 1.03$ GeV, respectively. Our prediction for the magnetic moment, $\mu_{\Xi^-} = -0.57\ \mu_N$, is close to the experimental value $-0.6507 \pm 0.0025\ \mu_N$ [40].

As is the case for the Λ hyperon, the calculations of ref. [31] predict a different sign and a smaller magnitude for the electric form factor of the neutral state of the Ξ doublet, but the other results agree very well.

The last point of our discussion concerns the form factors related to the $\gamma^* + \Sigma^0 \to \Lambda$ transition. We show the two form factors $F_1^{\Sigma\Lambda}(Q^2)$ and $F_2^{\Sigma\Lambda}(Q^2)$ in fig. 8, calculated with eqs. (28). The only link with experiment is the transition magnetic moment $|\mu_{\Sigma\Lambda}| = 1.61 \pm 0.08\ \mu_N$ from [40]. Our calculated value of $|\mu_{\Sigma\Lambda}| = 1.41\ \mu_N$ is about 15% off, but still reasonable considering the relatively large experimental error.

5 Conclusions

In this work, the first results of an extended implementation of the Bonn relativistic constituent-quark model into electromagnetic properties of the strangeness sector

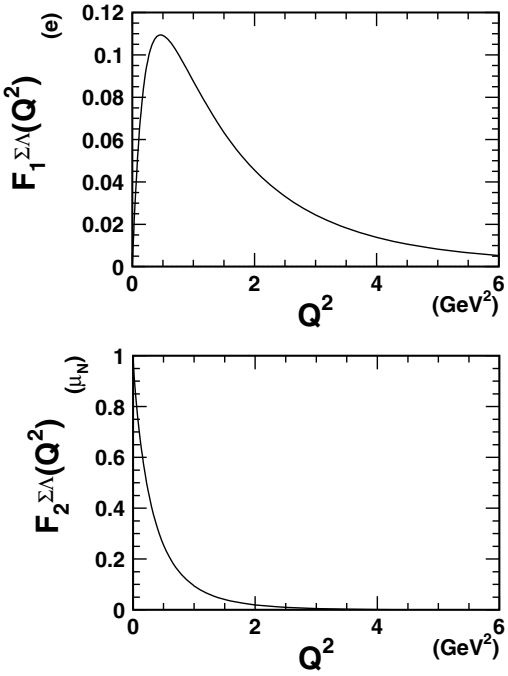

Fig. 8. The transition form factors of the $\gamma^* + \Sigma^0 \to \Lambda$ decay as defined in eq. (28).

have been presented. Electromagnetic form factors for the low-lying hyperons have been computed. Comparison with experimentally determined values is possible for the magnetic moments and the electric mean-square radius of the Σ^- hyperon. A nice agreement between our predictions and the data is observed. The predicted Q^2-dependence of the form factors is essential information when modeling kaon electroproduction processes within an isobar (or, hadrodynamic) framework [15]. As illustrated in sect. 4, to date the different hadron models do not even agree on the sign of the electric form factors of neutral hyperons. Some form factors have been observed to change sign at finite Q^2 values.

Work on calculating helicity amplitudes of known and *missing* hyperon resonances is in progress. We intend to conduct an elaborate investigation of strong decay widths of baryon resonances into the KY channels. In this way we hope to identify, on the basis of quark-quark dynamics, the most important intermediate baryon resonances in kaon photo- and electroproduction reactions.

References

1. M. Gell-Mann, Phys. Rev. **125**, 1067 (1962).
2. M. Gell-Mann, Phys. Lett. **8**, 214 (1964).
3. Y. Ne'eman, Nucl. Phys. **26**, 222 (1961).
4. G. Zweig, CERN Reports 8182/TH, 401 (1964), unpublished internal report.
5. G. Zweig, CERN Reports 8419/TH, 412 (1964), unpublished internal report.
6. Q. Zhao, Phys. Rev. C **63**, 025203 (2001).
7. Z. Li, B. Saghai, Nucl. Phys. A **644**, 345 (1998).
8. Y. Oh, A.I. Titov, S.N. Yang, T. Morii, Phys. Lett. B **462**, 23 (1999).
9. P. Kroll, M. Schürmann, K. Passek, W. Schweiger, Phys. Rev. D **55**, 4315 (1997).
10. T. Sato, T.-S.H. Lee, Phys. Rev. C **54**, 2660 (1996).
11. T. Yoshimoto, T. Sato, M. Arima, T.-S.H. Lee, Phys. Rev. C **61**, 065203 (2000).
12. S. Janssen, J. Ryckebusch, W. Van Nespen, D. Debruyne, T. Van Cauteren, Eur. Phys. J. A **11**, 105 (2000).
13. S. Janssen, J. Ryckebusch, D. Debruyne, T. Van Cauteren, Phys. Rev. C **65**, 015201 (2002).
14. S. Janssen, J. Ryckebusch, D. Debruyne, T. Van Cauteren, Phys. Rev. C **66**, 035202 (2002).
15. S. Janssen, J. Ryckebusch, T. Van Cauteren, Phys. Rev. C **67**, R052201 (2003).
16. D.S. Carman *et al.*, Phys. Rev. Lett. **90**, 131804 (2003).
17. R.G.T. Zegers *et al.*, Phys. Rev. Lett. **91**, 092001 (2003).
18. K.-H. Glander *et al.*, Eur. Phys. J. A **19**, 251 (2003) and private communication.
19. A. D'Angelo *et al.*, in *NSTAR 2001, Proceedings of the Workshop on the Physics of Excited Nucleons*, edited by D. Drechsel, L. Tiator, Vol. **347** (World Scientific, New Jersey, London, Singapore, Hong Kong, 2001).
20. R. Petronzio, S. Simula, G. Ricco, Phys. Rev. D **67**, 094004 (2003).
21. U. Löring, K. Kretzschmar, B. Metsch, H.-R. Petry, Eur. Phys. J. A **10**, 309 (2001).
22. U. Löring, B. Metsch, H.-R. Petry, Eur. Phys. J. A **10**, 395 (2001).
23. U. Löring, B. Metsch, H.-R. Petry, Eur. Phys. J. A **10**, 447 (2001).
24. D. Merten, *Hadron form factors and decays*, PhD Thesis, Rheinische Friedrich-Wilhelms-Universität Bonn, Germany (2002).
25. E.E. Salpeter, H.A. Bethe, Phys. Rev. **84**, 1232 (1951).
26. M. Koll, R. Ricken, D. Merten, B.C. Metsch, H.-R. Petry, Eur. Phys. J. A **9**, 73 (2000).
27. D. Merten, U. Löring, K. Kretzschmar, B. Metsch, H.-R. Petry, Eur. Phys. J. A **14**, 477 (2002).
28. R.F. Wagenbrunn, S. Boffi, W. Klink, W. Plessas, M. Radici, Phys. Lett. B **511**, 33 (2001).
29. M.I. Adamovich *et al.*, Eur. Phys. J. C **8**, 59 (1999).
30. SELEX Collaboration (I. Eschrich *et al.*), Phys. Lett. B **522**, 233 (2001).
31. H.-Ch. Kim, A. Blotz, M.V. Polyakov, K. Goeke, Phys. Rev. D **53**, 4013 (1996).
32. B. Kubis, T.R. Hemmert, U.-G. Meißner, Phys. Lett. B **456**, 240 (1999).
33. B. Kubis, U.-G. Meißner, Eur. Phys. J. C **18**, 747 (2001).
34. W. Plessas, *Nuclear Dynamics: From Quarks to Nuclei, Proceedings of the XXth CFIF Fall Workshop, Lisbon, Portugal*, edited by M.T. Pena, A. Stadtler, A.M. Eiro, J. Adam, Few-Body Syst. Suppl. **15**, 139 (2003).
35. L.Ya. Glozman, W. Plessas, K. Varga, R.F. Wagenbrunn, Phys. Rev. D **58**, 094030 (1998).
36. L.Ya. Glozman, Z. Papp, W. Plessas, K. Varga, R.F. Wagenbrunn, Phys. Rev. C **57**, 3406 (1998).
37. R.K. Bhaduri, L.E. Cohler, Y. Nogami, Nuovo Cimento A **65**, 376 (1981).
38. L. Theußl, R.F. Wagenbrunn, B. Desplanques, W. Plessas, Eur. Phys. J. A **12**, 91 (2001).
39. J.J. Kelly, Phys. Rev. C **66**, 065203 (2002).
40. K. Hagiwara *et al.*, Phys. Rev. D **66**, 010001 (2002).